Title
Bulk quantum Hall effect in eta-Mo4O11

Journal
SYNTHETIC METALS, 103(1-3)

ISSN
0379-6779

Authors
Hill, S
Brooks, JS
Uji, S
et al.

Publication Date
1999-06-01

DOI
10.1016/S0379-6779(98)00211-2

Synthetic Metals 103 (1999) 2667–2670

Bulk Quantum Hall Effect in η-Mo_4O_{11}

S. Hill [a], J.S. Brooks [b], S. Uji [c], M. Takashita [c], C. Terakura [c], T. Terashima [c], H. Aoki [c], Z. Fisk [b] and J. Sarrao [d]

[a] *Department of Physics, Montana State University, Bozeman, MT59717, USA*
[b] *National High Magnetic Field Laboratory, 1800 E. Paul Dirac Dr., Tallahassee, FL32310, USA*
[c] *National Research Institute for Metals, Tsukuba, Ibaraki 305, Japan*
[d] *Los Alamos National Labs, MST-10, Mail Stop K764, Los Alamos, NM87545, USA*

Abstract

We have observed a quantum Hall effect in the bulk quasi-two-dimensional conductor η-Mo_4O_{11}. The Hall resistance exhibits well defined plateaux, coincident with pronounced minima in the diagonal resistance. We present data for several different samples and contact geometries, and discuss a possible mechanism for the quantum Hall effect in this system. We also discuss the implications of these findings in the light of recent predictions concerning chiral metallic surface states in bulk quantum Hall systems.

Keywords: Magnetotransport, Hall effect, Superlattices

1. Introduction

In the realm of high magnetic fields, there is immense interest in the physics of low-dimensional conducting systems when the magnetic energy (orbital and Zeeman) becomes comparable to the electronic (Fermi) energy – *i.e.* the quantum limit. In a strictly two-dimensional (2D) electron system, it is well known that the quantum Hall effect (QHE) and the fractional QHE are observed under such conditions, so-called because the Hall conductance is quantized over extended intervals in magnetic field [1]. In a 2D quantized Hall phase, electronic states at the Fermi energy are Anderson localized within the bulk of the sample, while there exist extended states at the edges of the sample which are robust against scattering by disorder.

Hall resistance quantization has also been observed in bulk systems such as the organic Bechgaard salts [2]. Although strictly three dimensional, the electronic structures of these materials are highly anisotropic, or quasi one-dimensional (Q1D). Nevertheless, the basic ingredients which give rise to a QHE are essentially the same as those which give rise to the conventional 2D QHE, though the mechanisms are entirely different. In the Bechgaard salts, it is the remarkable properties of a field-induced-spin-density-wave which stabilize the QHE [3]. The quantized Hall resistance is brought about by Landau quantization of tiny residual pieces of Fermi surface left over from the imperfectly nested Q1D Fermi surface. These residual Fermi surfaces must be quasi two-dimensional (Q2D) in order for the magnetic field to produce clear mobility gaps in its electronic excitation spectrum (a prerequisite for the QHE). Meanwhile, the field-induced-spin-density-wave condensate plays the same role as the Anderson localized states in the conventional 2D QHE, by pinning the Fermi energy in these mobility gaps over extended intervals in magnetic field.

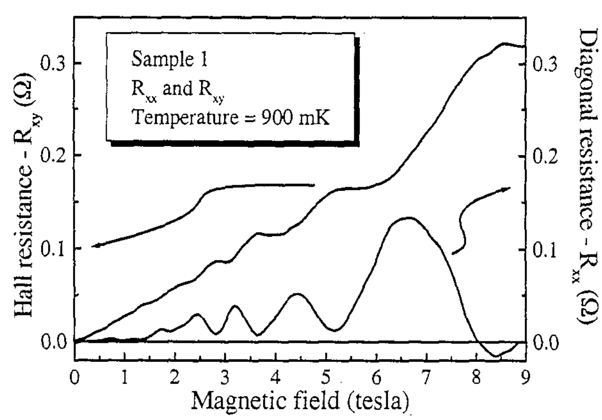

Fig. 1. Representative magnetotransport data for η-Mo_4O_{11}.

In this paper, we present convincing evidence for a bulk QHE in the inorganic charge-density-wave (CDW) conductor η-Mo_4O_{11}. Very deep minima (~ zeros) in the transverse diagonal resistance (R_{xx}) coincident with plateaux in the Hall resistance (R_{xy}) are observed, as illustrated in Fig. 1. This represents the first observation of the QHE in a truly bulk inorganic conductor.

In the light of these findings, and those of previous studies involving the Bechgaard salts, it is natural to compare and contrast the 2D and bulk QHEs. Indeed, recent theoretical studies predict the existence of a novel metallic surface sheath at the edge of a bulk quantum Hall conductor, analogous to the edge states in the conventional 2D QHE [4,5]. We make a legitimate case for η-Mo_4O_{11} as a viable system for gaining new insight to the properties of bulk quantum Hall systems.

PII: S0379-6779(98)00211-2

2. η-Mo_4O_{11}

The crystal structure of η–Mo_4O_{11} consists of layers of MoO_6 octahedra, parallel to (100), separated by MoO_4 tetrahedra, giving rise to a Q2D electronic structure [6]. The room temperature Fermi surface of η–Mo_4O_{11} has been calculated using a tight-binding method [7,8]; both electron and hole pockets elongated along the $\boldsymbol{a}^*$ axis are predicted, in agreement with recent experiments [9]. Within the ***bc*** plane, the electronic properties show considerable anisotropy, reflecting a "hidden" Q1D electronic character which is related to the presence of Q1D conducting chains along the $\boldsymbol{b}$ and $\boldsymbol{b} \pm \boldsymbol{c}$ crystallographic directions [8,10]. A consequence of this "hidden" one-dimensionality is that η-Mo_4O_{11} undergoes two successive CDW transitions, the first at 109 K followed by a second at ~30 K [6]. Each transition nests large sections of the room temperature Fermi surface leaving very small, highly two-dimensional, hole and electron pockets at low temperatures [11].

In a previous study, considerable insight into the ground state electronic structure of η-Mo_4O_{11} was achieved [11]. Indeed, the possibility of observing a quantum Hall effect was discussed. In particular, the striking similarity between η-Mo_4O_{11} and the semimetallic InAs/GaSb superlattice system with closely matched electron and hole densities was noted [12]. Both systems may be thought of as arrays of weakly coupled 2D electron systems. What is more, they have similar bandstructure parameters and mobilities. As a result, both materials undergo a field-induced transition to a semiconducting state when the quantum limit is reached and the hole and electron bands uncross [11]. It is these properties of η-Mo_4O_{11} which motivated the present study, namely, the possibility of observing a QHE in a truly bulk Q2D system in reasonable laboratory fields, *i.e.* < 20 tesla.

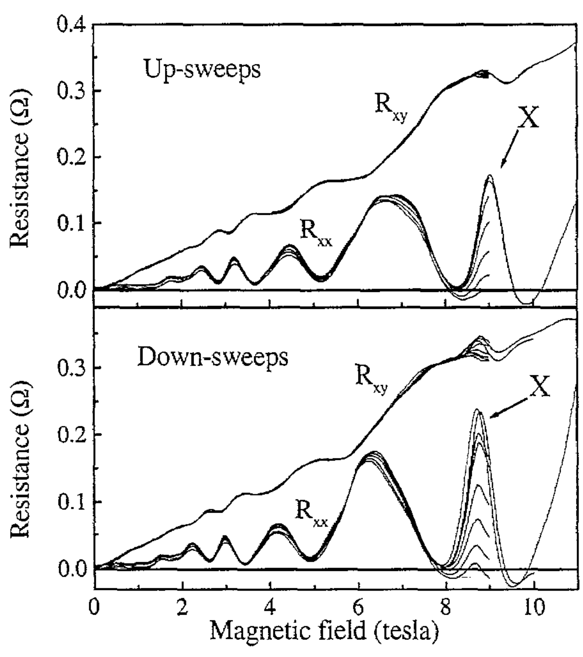

Fig. 2. Temperature dependence of R_{xx} and R_{xy} below 1 K (sample #1). The strongly temperature dependent features are artifacts (see text). The data were taken at more-or-less evenly spaced intervals in temperature from 900 mK to 70 mK; the lowest temperature data have the largest R_{xx} maxima.

3. Experimental details

Single crystals of η-Mo_4O_{11} were grown by a vapor-transport method [13]; they form as small platelets (~ $1 \times 0.5 \times < 0.1$ mm^3) with the platelet plane defined by the ***bc***-plane. Several different samples from two separate sample growths were studied, thereby providing a high level of confidence in our results. Resistance measurements were made using standard four terminal *a.c.* lock-in techniques through gold wires attached to the sample with conductive paint. Contact resistances were typically of the order of a few Ohms, and excitation currents in the range 50 μA (dilution fridge) to 200 μA (^{3}He fridge) were used.

For measurements of the in-plane (***bc***-plane) resistance tensor, four contacts were placed on the thin edges of the sample, while the longitudinal, or $\boldsymbol{a}^*$-axis resistance (R_{zz}), was measured by means of pairs of contacts on opposite faces of the plate-like samples. A current $I_{m,n}$ was then passed through the sample via contacts m and n, and a potential difference $V_{p,q}$ was measured across the sample between a different set of contacts p and q.

For in-plane measurements, the ratio $V_{p,q}/I_{m,n}$ yields a resistance which is an ad-mixture of both diagonal and off-diagonal components of the resistance tensor. These contributions may be separated according to the reciprocity principle [14]. Reversing the direction of the applied magnetic field changes the sign of the Hall voltage, but not the dissipative voltage. Thus, symmetric and asymmetric averages of the resistances measured with the magnetic field applied parallel and antiparallel to the $\boldsymbol{a}^*$-axis yield the diagonal and transverse Hall (R_{xy}) components of the resistance tensor respectively. This procedure is not necessary when measuring R_{zz}.

Experiments were carried out at the National High Magnetic Field Laboratory in Florida, and at the National Research Institute for Metals in Tsukuba, Japan. The majority of the measurements were conducted in superconducting solenoids and dilution refrigerators, though resistive magnets and a ^{3}He refrigerator were also employed for some experiments.

4. Experimental results

Fig. 2 shows a series of measurements of R_{xx} and R_{xy} for sample #1, at temperatures below 1 K. Plateaux in R_{xy} can clearly be seen at fields of ~3, 4, 5.5 and 8-10 T. For the most part, the temperature dependence of R_{xy} is very weak, except at ~9 T. Similarly, the temperature dependence of R_{xx} is weak except in the vicinity of 9 T. This temperature dependence (at 9 T), and the irregular form of the highest field R_{xy} plateau, are experimental artifacts which are discussed further below.

It is apparent from Fig. 2 that there is considerable hysteresis between up- and down-sweeps of the magnetic field. This is well known for this material and has been attributed to pinning of a field dependent CDW [11]. Unfortunately, this affects the averaging technique used to obtain R_{xx} and R_{xy}, which may explain the rounding off of the Hall plateaux and the deviations from perfect zeros in R_{xx}. However, the field dependence of the CDW turns out to be an essential ingredient for the existence of a QHE in η-Mo_4O_{11}.

Fig. 3 shows the temperature dependence of R_{zz} obtained over a similar temperature range as the data in Fig. 2, though for a different sample (#2); this data is consistent with all previous measurements of R_{zz} [11]. Superimposed on this figure is some of the data in Fig. 2. It is immediately apparent that the strongly temperature dependent feature in Fig. 2 (labeled X) is correlated with the R_{zz} peak at 9 T in Fig. 3. Not surprisingly, the symmetric

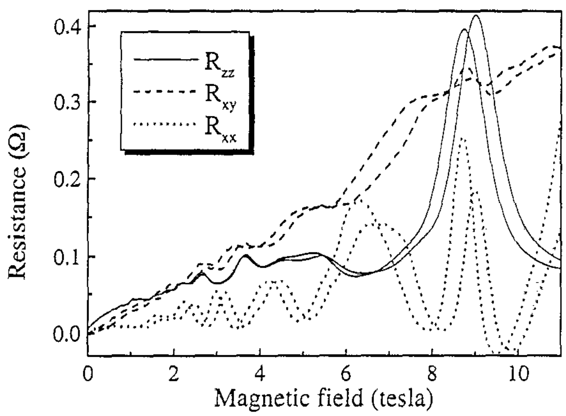

Fig. 3. Temperature dependence of R_{zz} (sample #2). The 100 mK R_{xx} and R_{xy} data from Fig. 2 is included for comparison.

average is unable to separate the longitudinal (R_{zz}) and transverse (R_{xx}) diagonal components of the resistance tensor. Possible explanations as to why R_{zz} shows up in a measurement of R_{xx} will be discussed in the following section. Nevertheless, the independent measurement of R_{zz} provides an alternative means of distinguishing between R_{zz} and R_{xx}. Removal of R_{zz} reveals a broad minimum (~zero) which is coincident with a region where the slope of R_{xy} is extremely shallow, *i.e.* plateau-like – this is shown in Fig. 4.

Above 11 T, R_{xx} increases sharply, while the slope of R_{xy} changes sign. This behavior is consistent with our earlier work (ref. [11], see also Fig. 5) and is associated with the transition to a semiconducting state. Incidentally, the earlier measurements were performed on thicker samples; the Hall resistance, at 9 T, in the present sample is more than an order of magnitude greater than in previous studies, which probably explains why well defined R_{xy} plateaux and R_{xx} minima have not been observed until now. The reason for the poorly quantized Hall resistance at 9 T may be attributed to increased hysteresis and the fact that R_{xx} increases sharply above 9 T. These factors, together with the strongly temperature dependent ad-mixture of R_{zz} in the raw signal, greatly increase the uncertainty in the asymmetric averaging method used to obtain R_{xy} above about 8 T.

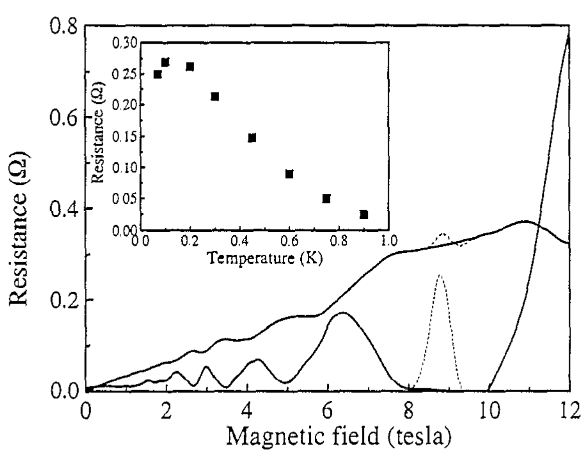

Fig. 4. Corrected R_{xy} and R_{xx} data for sample #1 at 100 mK. The inset shows the temperature dependence of the resistance peak attributed to R_{zz} at 9 T (dashed line in main part of figure).

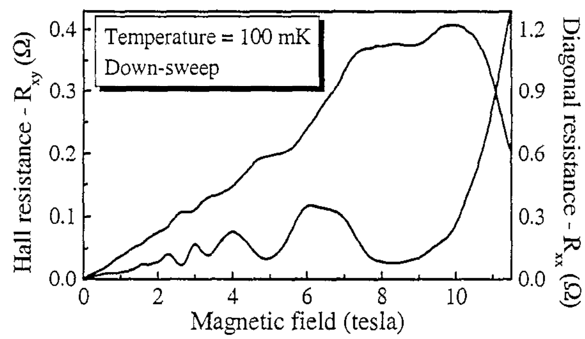

Fig. 5. R_{xy} and R_{xx} data for sample #3.

The inset to Fig. 4 shows the temperature dependence of the 9 T R_{zz} resistance maximum. Previous studies have indicated that R_{zz} is activated in the vicinity of 9 T, at temperatures above about 500 mK [11]. The present data indicate that R_{zz} tends to saturate and even decrease somewhat below about 300 mK. The possible significance of this will be discussed in the following section.

Fig. 5 shows raw R_{xy} data for sample #3 which is in good agreement with the data in Figs. 2 and 4. Sample #3 was cleaved from the same polycrystal as sample #1. It is interesting to note that the absolute Hall plateau resistances at ~9 T are similar for Samples #1 and #3, *i.e.* ~ 0.32 Ω and 0.38 Ω respectively [Note: these values are averages from many measurements with errors of ± 5 mΩ]. These resistances should scale inversely with the thickness' of the two samples which, indeed, turns out to be the case to within the experimental error. The thickness' of samples #1 and #3 are 50 and 40 μm (± 5 μm) respectively.

In order to determine the filling factor corresponding to each Hall plateau, we plot the inverse of R_{xy}, for a fourth sample (#4), against inverse magnetic field (Fig. 6). Again, well defined plateaux are observed and, as with sample #1, there is no discernible temperature dependence in R_{xy}. The data has been normalized with respect to the 9 T Hall plateau in order to demonstrate that quantization occurs in units of the 9 T Hall conductance, *i.e.* when normalized and plotted in this way, plateaux occur at integer multiples of the 9 T Hall conductance. However, it is apparent that the Hall plateaux do not occur at regular intervals in inverse magnetic field. This latter observation is rather anomalous and may be attributed to the field dependence of the CDW.

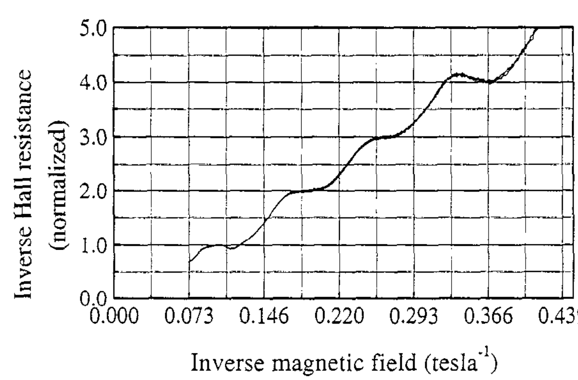

Fig. 6. Hall effect data for sample #4 at 125, 220 and 400 mK (over-laid). R_{xy}^{-1} has been normalized to its value at 9 T in order to demonstrate the excellent quantization.

Finally, we compare our measured Hall resistances with the fundamental Hall resistance quanta h/e^2 – the Klitzing. Taking as an example sample #3, which has a thickness of $40 \pm 5\ \mu$m, and assuming a value for $\boldsymbol{a}$ of 24.5 Å, one can deduce that a maximum of ~ 16,330 layers contribute to the measured Hall voltage. Thus, for filling factor $\nu = 1$, the minimum possible value for the Hall resistance is $1.58 \pm 0.2\ \Omega$ which, to within the experimental error, is four times the measured value.

5. Discussion

First, we discuss a possible mechanism for the bulk QHE in η-Mo_4O_{11}. Our previous investigations have determined that the ground state Fermi surface is highly 2D – one pre-requisite for the QHE [11]. Therefore, all that is required is some means of pinning the chemical potential between Landau bands over extended intervals in magnetic field. This can be achieved by any reservoir of immobile states which is capable of exchanging carriers with the mobile 2D states. Clearly it is the CDW which plays this role in η-Mo_4O_{11}, as evidenced by the hysteresis, which indicates that the CDW wavevector shifts upon application of a magnetic field. In fact, this effect is quite dramatic and accounts for the decrease in periodicity of the Hall steps with decreasing field, as seen in Fig. 6. This is a beautiful demonstration of the fact that carrier density has absolutely nothing to do with the QHE apart from fixing the positions of the Hall plateaux in field.

The above explanation suggests that the QHE is a natural property of imperfectly nested density-wave conductors. Indeed, indirect evidence exists for a QHE in some of the Q2D organic charge-transfer salts with spin-density-waves [15,16].

We next turn to the maximum observed Hall resistance, which corresponds to one quarter of a Klitzing per 2D layer. Accounting for a factor of two is trivial if the spin degrees of freedom within each Landau band are not resolved [1]. To explain the factor of four requires the introduction of an additional degeneracy of two among the electronic states of the system. It is quite possible that such a degeneracy could arise if there were two identical Fermi surfaces at different positions in the re-constructed Brillouin zone.

For the QHE to be observed at all, the Q2D Landau bands must be resolved from each other. In η-Mo_4O_{11}, the high degree of two-dimensionality, low carrier effective masses (~ 0.1 m_e) and a high mobility create these necessary conditions. The low effective mass leads to a cyclotron splitting between the centers of adjacent Landau bands of ~1 meV per tesla. From these numbers, and from the widths of the transitions between Hall plateaux (Fig. 2), we estimate the $\boldsymbol{a}$*-axis bandwidth to be ~1 meV ($\cong 10\ k_B$). Although very low, this value explains the non-resolution of spin-splitting and the weak temperature dependence of the data. Estimates of the g-factor in η-Mo_4O_{11} indicate that it is considerably less than the free electron value $g = 2$ [17]. Thus, the spin splitting can be expected to be considerably less than 1 meV, even at 9 T. In hindsight, it is clear that little temperature dependence in the data should be expected until the temperature is of the order of a few kelvin. Thus, the QHE in η-Mo_4O_{11} should persist to fairly high temperatures.

Turning to R_{zz}: the strong temperature dependence at 9 T is indicative of the fact that the bulk of the sample is completely insulating. There is beautiful agreement between R_{xx}, R_{xy} and R_{zz} at this point (Fig. 3), where peaks in R_{zz} coincide perfectly with the Hall plateaux. The reason for the minima in R_{xx} at these instances is not related to what is happening in the bulk of the sample, which is insulating, but to the sample edges where dissipationless edge channels supposedly reside. Away from the Hall plateaux R_{xx} increases due to dissipation in the bulk of the sample, while R_{zz} decreases as a result of the Fermi level coinciding with states which are mobile along the $\boldsymbol{a}$*-axis.

The reason for the admixture of R_{zz} and R_{xx}, as seen for the in-plane measurements in Fig. 2, is most probably due to imperfect contacts to the sample. Ideally, these contacts should connect to every layer. However, in practice, currents may flow between layers in order to reach other layers which are not well connected to the contacts. At first sight, this may seem undesirable. However, since R_{xx} is, in principle, zero whenever R_{zz} is maximum, this presents an extremely effective way of measuring R_{zz} close to the edges of the sample when the bulk of the sample is insulating. This ties in nicely with recent predictions concerning the transport of current along the a*-axis via edge states [4,5].

Balents and Fisher predict that, in layered samples which exhibit a bulk QHE, a 2D chiral metallic ribbon should exist at the edge of the sample [4]. It is expected that, at low temperatures, this surface layer should dominate the z-axis transport (*i.e.* parallel to the field) once the bulk of the sample becomes insulating. We propose that this may be one possible explanation for the saturation of R_{zz} at low temperatures, as seen in Fig. 4. Indeed, in the limit $T \rightarrow 0$, R_{zz} due to such a surface sheath is expected to become temperature independent.

7. Summary

We present convincing evidence for a bulk QHE in η-Mo_4O_{11}. We show data for several different samples and contact geometries, and discuss a possible mechanism for the QHE in this system. We also discuss possible implications of our results in the light of recent predictions concerning chiral metallic surface states in bulk quantum Hall systems.

This work was supported by NSF-DMR 95-10427 and in part by NSF cooperative agreement No. 98-71922. The NHMFL is supported by NSF cooperative agreement No. DMR-95-27035.

8. References cited

[1] T. Chakraborty and P. Pietilainen, *The Quantum Hall Effects-Fractional and Integer, Springer Series in Solid-State Sciences* **85** (Berlin, 1995).
[2] S. T. Hannahs *et al.*, Phys. Rev. Lett. **63**, 1988 (1989).
[3] P. M. Chaikin *et al.*, Physica B **177**, 353 (1992).
[4] L. Balents & M. Fisher, Phys. Rev. Lett **76**, 2782 (1996).
[5] J. Chalker & A. Dohmen, Phys. Rev. Lett **76**, 4496 (1996).
[6] *Low Dimensional Electronic Properties of Molybdenum Bronzes and Oxides*, edited by C. Schlenker (Kluwer, Dordrecht 1989); and references therein.
[7] E. Canadell *et al.*, *J. Inorg. Chem.*, **28**, 213 (1989).
[8] E. Canadell and M. Whangbo, *Chem. Rev.* **91**, 965 (1991).
[9] M. Sasaki *et al.*, Phys. Rev. B **47**, 6216 (1993).
[10] M. H. Whangbo *et al.*, *Science* **252**, 96 (1991).
[11] S. Hill *et al.*, Phys. Rev. B **55**, 2018 (1997).
[12] M. S. Daly *et al.*, Phys. Rev. B **53**, R10524 (1996).
[13] M. Inoue *et al.*, *Phys. Stat. Sol.* (b) **148**, 659 (1988).
[14] H. H. Sample *et al.*, *J. Appl. Phys.* **61** (3), 1079 (1987).
[15] N. Harrison *et al.*, Phys. Rev. Lett. **77**, 1576 (1996).
[16] S. Hill *et al.*, Phys. Rev, B **55**, R4891 (1997).
[17] S. Hill *et al.*, to be published.